

Electron-bombarded $\langle 110 \rangle$ -oriented tungsten tips for stable tunneling electron emission

T. K. Yamada, T. Abe, N. M. K. Nazriq, and T. Irisawa

Citation: *Review of Scientific Instruments* **87**, 033703 (2016); doi: 10.1063/1.4943074

View online: <http://dx.doi.org/10.1063/1.4943074>

View Table of Contents: <http://scitation.aip.org/content/aip/journal/rsi/87/3?ver=pdfcov>

Published by the [AIP Publishing](#)

Articles you may be interested in

[Field electron emission properties from zinc oxide nanostructures](#)

AIP Conf. Proc. **1502**, 426 (2012); 10.1063/1.4769161

[Note: Electrochemical etching of sharp iridium tips](#)

Rev. Sci. Instrum. **82**, 116105 (2011); 10.1063/1.3662473

[Refined tip preparation by electrochemical etching and ultrahigh vacuum treatment to obtain atomically sharp tips for scanning tunneling microscope and atomic force microscope](#)

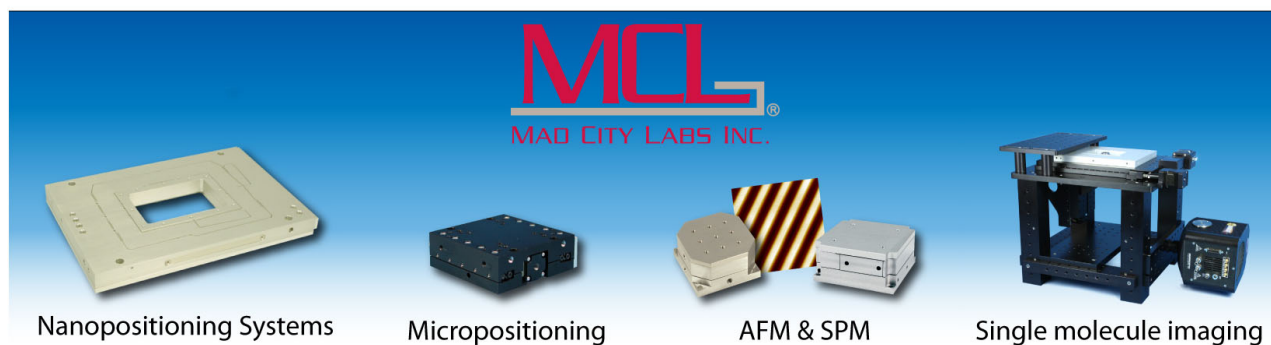
Rev. Sci. Instrum. **82**, 113903 (2011); 10.1063/1.3660279

[The effects of size and orientation on magnetic properties and exchange bias in Co₃O₄ mesoporous nanowires](#)

J. Appl. Phys. **109**, 07B520 (2011); 10.1063/1.3548831

[Ferroelectric and pyroelectric properties of highly \(110\)-oriented Pb \(Zr 0.40 Ti 0.60 \) O₃ thin films grown on Pt/La Ni O₃/Si O₂/Si substrates](#)

Appl. Phys. Lett. **90**, 232908 (2007); 10.1063/1.2746949



Electron-bombarded $\langle 110 \rangle$ -oriented tungsten tips for stable tunneling electron emission

T. K. Yamada, T. Abe, N. M. K. Nazriq, and T. Irisawa

Graduate School of Advanced Integration Science, Chiba University, 1-33 Yayoi-cho, Inage-ku, Chiba 263-8522, Japan

(Received 24 August 2015; accepted 18 February 2016; published online 11 March 2016)

A clean tungsten (W) tip apex with a robust atomic plane is required for producing a stable tunneling electron emission under strong electric fields. Because a tip apex fabricated from a wire by aqueous chemical etching is covered by impurity layers, heating treatment in ultra-high vacuum is experimentally known to be necessary. However, strong heating frequently melts the tip apex and causes unstable electron emissions. We investigated quantitatively the tip apex and found a useful method to prepare a tip with stable tunneling electron emissions by controlling electron-bombardment heating power. Careful characterizations of the tip structures were performed with combinations of using field emission I–V curves, scanning electron microscopy, X-ray diffraction (transmitted Debye-Scherrer and Laue) with micro-parabola capillary, field ion microscopy, and field emission microscopy. Tips were chemically etched from (1) polycrystalline W wires (grain size ~ 1000 nm) and (2) long-time heated W wires (grain size larger than 1 mm). Heating by 10–40 W (10 s) was found to be good enough to remove oxide layers and produced stable electron emission; however, around 60 W (10 s) heating was threshold power to increase the tip radius, typically $+10 \pm 5$ nm (onset of melting). Further, the grain size of ~ 1000 nm was necessary to obtain a conical shape tip apex. © 2016 AIP Publishing LLC. [<http://dx.doi.org/10.1063/1.4943074>]

INTRODUCTION

Many sharp and robust tips have been fabricated by using tungsten (W), which is remarkable for its high melting temperature of 3653 K and extraordinary hardness. Such W tips were first used as an electron source of field emission microscopy (FEM) in ultra-high vacuum (UHV).¹ By introducing inert gas, in 1950s, atomic structures of these W tips were successfully visualized.² Today, W tips are used for a variety of purposes: as an electron beam source for field-emission-type scanning electron microscopy (SEM),³ as a probe for scanning tunneling microscopy (STM) as well as atomic force microscopy (AFM),⁴ as an electron beam source for low-energy electron diffraction (LEED),⁵ as an ultrafast electron pulse source,⁶ and as a substrate tip for metal film coatings such as gold⁷ and magnetic films,⁸ because W does not mix with the coated metals.

Atomically sharp W tips have been developed intensively during the last decades, and many techniques have been reported. Starting from the aqueous etching,^{9–13} further treatments in UHV have been studied, such as self-sputtering,^{14,15} field evaporation,^{16,17} field-assisted etching,^{18,19} ion milling,²⁰ and controllable crashing.²¹ STM or SEM require not only satisfactory spatial resolution owing to sharpening of the tip apex but also stable tunneling electron emission, which is determined by the local density of states (LDOS) near the Fermi energy at the surface of the tip apex. Because local atomic symmetry at the tip apex determines the apex LDOS differently from the bulk bcc tungsten density of states (DOS), a tip with unchanged atomic morphology and electronic states under the application of strong electric field must be necessary for obtaining a stable electron source. We show

how unstable electron-emission tips cause troubles in STM and scanning tunneling spectroscopy (STS) measurements. Figures 1(a)–1(d) show the STM measurements performed on a clean and atomically flat Cu(111) surface with stable and unstable W tips. During the STM, a strong electric field of 10^6 – 10^{10} V/m is typically applied between the tip and sample. With stable tips, emission of tunneling electrons from the tip is maintained at constant level during the STM measurements. Therefore, a clear topographic image as well as a reliable dI/dV spectroscopic curve is obtained, as shown in Figs. 1(a) and 1(b), in which atomic terraces and Shockley-type surface state around -400 meV, respectively, can be observed. On the other hand, an unstable tip yields time-variable tunneling electron emission. Therefore, the obtained topographic image shown in Fig. 1(c) reveals several tip-changes (marked by the arrows) and many drops from the tip (marked by the circles). The dI/dV curve, shown in Fig. 1(d), reveals spiky noise in the curve (a sudden movement of the apical atom changes the tip-sample distance; thus, the dI/dV value jumps, $dI/dV \propto \rho \exp(-2\kappa z)$, where ρ : LDOS and κ : decay coefficient, and z : tip-sample distance), owing to very strong electric fields. Important considerations for achieving stable tunneling electron emission are (1) removal of impurity films, such as oxide films, with which the W tip apex is coated after aqueous etching and (2) construction of a robust apex crystalline structure (atomic planes) yielding stable LDOS at the apex (sufficiently tough to withstand strong electric fields). Atomically sharp tips may not be good for achieving stable tunneling electron emission because adatoms or atomic steps on the apex could be moved by the strong electric field due to weaker coordination.

Effective treatments for removal of the oxide films at the W apex have been reported: hydrofluoric acid etching

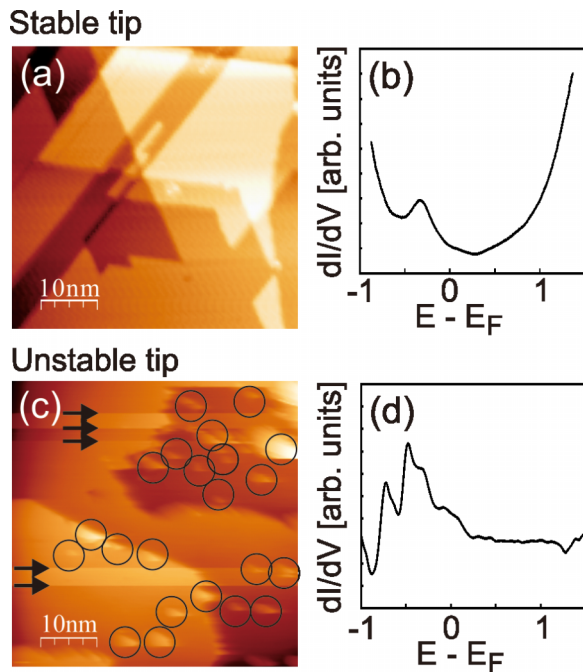


FIG. 1. STM topographic images and obtained dI/dV curves on a clean and atomically flat Cu(111). (a) and (b) were obtained with a stable W tip and (c) and (d) were obtained with an unstable W tip. (a) and (c) show STM topographic images (50×50 nm) (a) $V_s = -1$ V, $I = 350$ pA, (c) $V_s = +2$ V, $I = 150$ pA), and (b) and (d) show the dI/dV curves ($V_s = 1$ V, $I = 1$ nA). In (c), the arrows and circles denote tip-change positions and drops from the tip, respectively.

in air, self-sputtering in UHV, and proper heating in UHV. Hydrofluoric acid etching is useful for removing very thick oxide films (several tens of nm).²² This treatment is performed in air, and the etched tip is exposed to air; thus, slight oxidization of the tip surface cannot be avoided. By using self-sputtering, the apical oxide films can be removed because ions that are accelerated toward the apex preferentially hit the tip part located ~ 10 nm from the apex, creating a neck and eventually removing the apex (~ 10 nm in size).^{15,23} Because this process is performed in UHV, the obtained W apex is bare tungsten, while the surface structure is affected by the sputtering; thus, the tip apex atomic plane and LDOS are unclear. Another effective treatment for removal of the apical oxide films is heating. Heating to 1000–2200 K in UHV has been reported.^{16,20,24,25} However, measuring the temperature at the tip apex is very difficult; thus, the reported heating temperatures vary from reference to reference. According to the empirically known resistive heating process,¹⁶ first a W tip is contacted or spot-welded with a conductive wire, following which a current is flown through the wire. By monitoring the glow of the wire, the tip temperature can be controlled (dark red glow corresponding to 900 K, orange glow corresponding to 1175–1300 K, yellow glow corresponding to 1375 K),¹⁶ while the apex temperature remains unknown.

In this study, we investigated the heating treatment of a W tip apex in UHV, for removal of impurity films from the tip apex surface and for generating robust atomic planes that can endure strong electric fields for obtaining stable tunneling electron emission. Characterizations of the tip apex were carefully performed with combinations of using field

emission I–V curves, SEM, X-ray diffraction (transmitted Debye-Scherrer and Laue) with micro-parabola capillary, field ion microscopy (FIM), and FEM and found that electron-bombardment heating by 10–40 W (10 s) was good enough to remove oxide layers and produced stable electron emission; however, around 60 W (10 s) heating was the threshold power to increase the tip radius, typically $+10 \pm 5$ nm (onset of melting). Further, the grain size of ~ 1000 nm was necessary to obtain a conical shape tip apex.

EXPERIMENTAL

The W tip was prepared in a simple and quick manner, as follows. In air, the tip was etched from a W wire with aqueous KOH and cleaned by HF acid. Subsequently, the tip was introduced into an UHV chamber. Tips were chemically etched from (1) polycrystalline W wires and (2) long-time heated W wires. All X-ray measurements were performed in air. STM and STS were performed in an analysis chamber of our home-build UHV-STM setup (5×10^{-8} Pa), while tip-heating, field emission I–V curves, and FEM/FIM measurements were performed in a preparation chamber of the same UHV-STM setup; thus without breaking UHV, we checked the tip apex. The shape of the tip apex was checked by using a commercial SEM setup (Tiny SEM, Technex, 10^{-3} Pa).

In this study, to check the stability of the electron emission from the tip apex, field emission I–V curves were measured (sharper tips emitted electrons at lower voltages). Figure 2(a) shows our field emission curve measurement setup, located inside the preparation chamber of our UHV STM setup. The filament (W, diameter of 0.15 mm) was degassed well until the pressure kept the base pressure during the current flow. The field emission curves are useful for measuring the radii inside the UHV preparation chamber in the STM setup. In UHV, a counter electrode (W filament) was set 1 mm away from the tip apex. Field-emitted electrons were detected by the counter electrode (I–V curve), when electric field in the 10^6 – 10^7 V/m range was applied between the anode filament and the cathode tip. The maximal negative applied bias voltage was 3 kV, i.e., tip radii of up to 150 nm could be checked, while FIM/FEM allows measuring only sharp tips ($r < 10$ nm). Bias voltages above 3 kV frequently damaged the apexes by sparking owing to the tip apex contaminations. Our LabVIEW program stopped the voltage application when the counter electrode detected the set current of 5 nA, and automatically saved the data. The two I–V curves obtained from the same tip apex are shown as dots in Fig. 2(b), which were compared with the Fowler–Nordheim equation.¹⁵ By following Ref. 15, field emission current can be described as $I = 1.537 \times 10^{-14} \times \frac{2\pi^2 F^2}{\phi t(y)^2} \exp\left(\frac{-0.683\phi^{1.5}}{F} \omega(y)\right)$, $t(y) = 0.9967 + 0.0716y + 0.0444y^2$, $\omega(y) = 1.0029 - 0.1177y + 1.1396y^2 - 0.2561y^3$, $y = 3.79F^{1/2}/\phi$, $F = V/5r$, where d , distance between the apex and the counter electrode, 1 mm, and r , tip radius. We assumed the work function of $\phi \sim 5.5$ eV for a W(110) plane.²⁶ Our I–V measurement setup has a current noise of ~ 50 pA, which is shown as error bars in Fig. 2(b). The simulated I–V curves are shown as solid lines in Fig. 2(b), where the lower panel is shown in a log-scale. Blue and black lines denote simulated

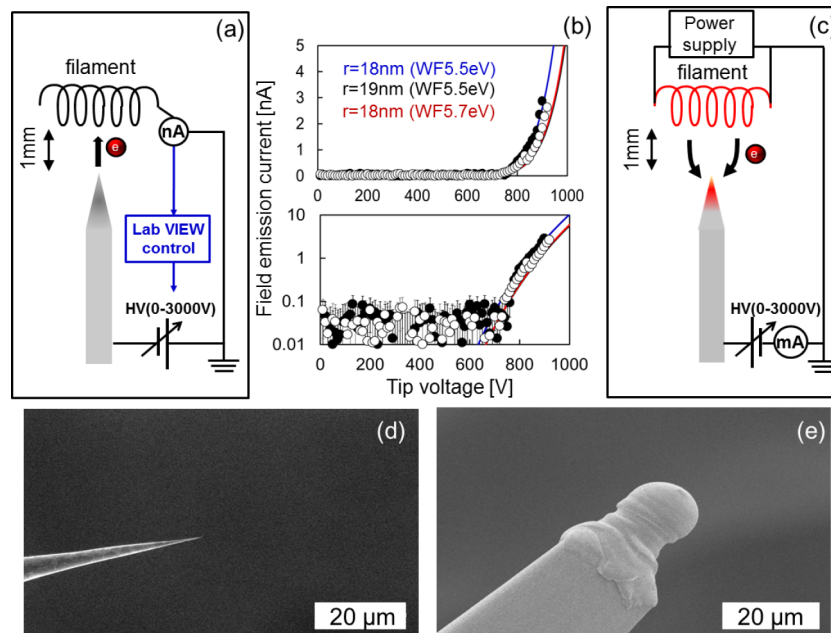


FIG. 2. (a) A sketch of our field emission I-V measurement setup in UHV chamber. (b) Black and white dots denote field emission I-V curves experimentally obtained from the same tip. Black, blue, and red solid lines are simulated I-V curves for $r = 18$ nm (WF: 5.5 eV), 19 nm (WF: 5.5 eV), and 18 nm (WF: 5.7 eV), respectively. For sharper tips, the emission curves shift toward lower voltages. (c) A sketch of our electron-bombardment measurement setup without changing the layout from (a). (d) and (e) show SEM images of a sharp W tip and a melted W tip owing to high heating power, respectively.

lines when the tip radius, r , is 18 and 19 nm, respectively, with a work function of 5.5 eV. The red line was simulated with the same tip radius as the blue line, i.e., 18 nm, but the work function is 5.7 eV. Since the black and the red lines are almost identical, increasing the tip radius of +1 nm is comparable to increasing the work function of +0.2 eV. In this study, we assumed the work function of 5.5 eV,²⁶ since our X-ray studies confirmed a bcc-W(110) plane at the apex (the atomic plane larger than 5 nm), and it is hard to believe that the increase of the work function much more than 5.5 eV at the W(110) apex. From the comparisons in Fig. 2(b), we can determine the tip radius with an accuracy of ± 1 nm, i.e., the tip in Fig. 2(b) could have a radius of 18.5 ± 0.5 nm. We use this method to evaluate the tip radius.

The tips after introducing into the UHV preparation chamber were heated. Figure 2(c) shows our electron bombardment heating setup. Without changing the tip and the counter electrode (W filament) positions (the same as Fig. 2(a)), we passed a current through the filament and applied a positive bias (+1 kV) to the tip, where the filament's hot electrons predominantly heat the apex because the electrical flux lines concentrate toward the apex. Heating was controlled with three parameters: (1) thermal power (W) = hot electrons (mA) \times applied positive voltage (kV), (2) time (s), and (3) number of repetitions. During the heating process, we set the constant voltage, e.g., +1 kV. We changed the filament current and controlled the emission current from the filament; thus we controlled the heating power. For example, at +1 kV, emission current of 40 mA gives 40 W. We lasted the heating only for 10 s to avoid extra impurities desorbing from the surroundings of the tip apex. By using the same setup as in Fig. 2(a), we can smoothly repeat the I-V measurements and heating treatment. Heating by electron bombardment has been frequently used to increase the tip temperature up to 2200 K, while a relatively

large heating power was required. Because the filament is set in front of the tip apex, an infrared pyrometer cannot be used for precisely measuring the tip apex temperature. The W tip apex can melt if the heating is too strong. Figures 2(d) and 2(e) demonstrate the results. First, we prepared a sharp etched W tip, shown in Fig. 2(d), and repeatedly heated it in UHV, by using a power of 50-100 W for more than 10 s. The tip was transferred into the STM without halting the UHV and was approached to the sample. However, no clear STM topographic images were obtained. Thus, the tip was removed from the UHV STM and the apex was checked by using SEM. Figure 2(e) shows the result of this test. The tip apex melted. With this extra-blunt tip, tunneling current was emitted from multiple points on the tip apex surface (unstable), and no clear STM image could be obtained. Therefore, in this study, we investigated the proper heating power for removal of impurity films without making the tip blunter and unstable emission. To avoid complete melt, in this study, we used a heating time of 10 s.

RESULTS AND DISCUSSION

First, we characterized the tips etched from a commercial W polycrystalline wire (purity 99.9%). It is known by FEM/FIM that even polycrystalline wire, the etched tip has a (110) plane. We confirmed the origin of this (110) plane appearance by using X-ray measurements. Figure 3(a) shows an X-ray image (transmitted Debye-Scherrer) obtained from the W polycrystalline wire. In spite of the polycrystalline, X-ray image shows not only Debye-rings but also several spots, which shows that the W wire had a $\langle 110 \rangle$ orientation along the wire axis. The reason could be the wire drawing process. We chemically etched the wire and obtained the tip (SEM image

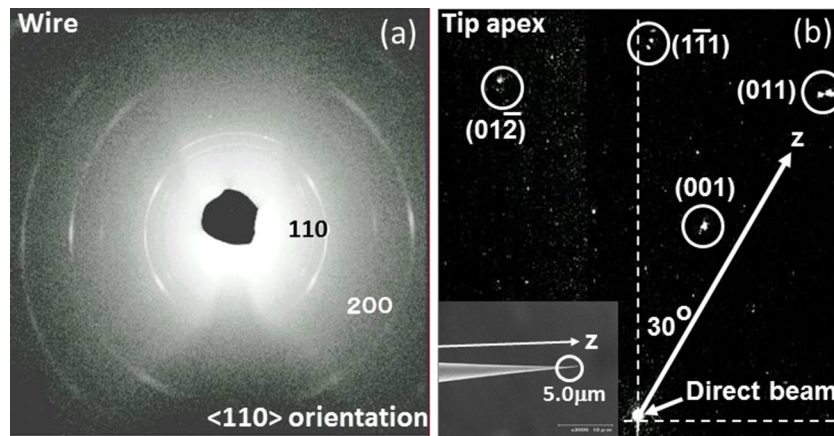


FIG. 3. (a) Transmission type X-ray Debye-Scherrer image obtained from a commercial polycrystalline W wire. (b) X-ray Laue image obtained from the tip apex by illuminating the 5000 nm region with micro-parabola capillary. The inset shows the tip's SEM image. All data were obtained by using an X-ray W tube, 40 kV, 20 mA, exposure time of 120 min. During the measurements, the W wire rotated around the fixed z-axis.

in inset to Fig. 3(b)). By using the micro-parabola capillary, the X-ray was projected only onto the tip apex (~ 5000 nm). The obtained X-ray Laue image (Fig. 3(b)) now shows no Debye-rings, but sharp spots, suggesting that the tip apex is single-crystallized, even without any heating, and the $\langle 110 \rangle$ direction is parallel to the wire axis, with possible deviation contained within 5° . In Fig. 3(b), four spots can be observed (contained within the white circles), indicating four 1000-nm-size grains at the apex. This can explain why the FIM/FEM images obtained from the tip etched from the polycrystalline wire exhibit a (110) plane at the apex.⁸

Next, the tip etched from the polycrystalline wire was set into the UHV chamber and the field emission I-V curves were measured. We measured three times as shown in Fig. 4(a); however, the obtained I-V curves varied. This variability can be attributed to adsorbed molecules or impurity layers on the tip apex surface. After heating the unstable tip in Fig. 4(a) by 10 W ($10 \text{ s} \times 1$), the obtained I-V curves in Fig. 4(b) suggested good reproducibility, indicating that unstable surface layers were removed and a stable W metal surface was exposed. The three I-V curves suggested the tip radius of 18 nm. During the heating between Figs. 4(a) and 4(b), the pressure increased from 10^{-8} Pa to 10^{-7} - 10^{-6} Pa. If the residual gases were ionized, the residual gas ions might also sputter the tip apex and therefore the tip radius could become sharper. We increased the heating power up to 36 W ($10 \text{ s} \times 1$) and obtained the I-V curves identical to those in Fig. 4(b), indicating no change at the apex. We also tested these heating treatments in several different setups, but in keeping the tip-sample separation of ~ 1 mm with W filaments with a diameter of 0.15 mm, we always get the emission current of 10-40 mA by applying the bias of +1 kV and the filament current of typically 2.0-2.3 A. These parameters will be useful for many researchers who need stable W tips.

Now we are curious to check the threshold power, which start to change the apex and increase radius (make blunter) and finally complete melt (like Fig. 2(e)). In Figs. 4(c) and 4(d), we investigated the threshold heating power. Lower panels show in a log-scale. Solid lines are experimentally obtained I-V curves, and the dashed lines are fitted curves. Figure 4(c) shows the I-V curves obtained for another W

tip with the radius of 17 nm after annealing it up to 36 W ($10 \text{ s} \times 1$). Again, the I-V curve measurements were repeated three times, suggesting good reproducibility and thus stable W apex fabrication. To determine the threshold power, we further increased the power. After heating by 40 W, 50 W, and 55 W, there were no changes in the I-V curves. Each heating cycle lasted 10 s. We repeated the heating three times ($10 \text{ s} \times 3$); however, the I-V curves remained the same. Finally, by using a 58 W ($10 \text{ s} \times 1$) annealing power, we managed to increase the tip radius to 26 nm, as shown in Fig. 4(d). We tested several W tips made from polycrystalline W wires and found the threshold heating power of ~ 60 W for obtaining the tip blunter (typically, by 60 W, the tip radius increases by $+10 \pm 5$ nm).

Our study confirmed that only one heating with a power of 10-40 W lasting 10 s is sufficient for obtaining a stable W tip apex, producing a stable electron emission. An additional finding from this study is that gentle heating at about 60 W ($10 \text{ s} \times 1$) can change the apex blunter. Typically, the tip radius increased with $+10 \pm 5$ nm, which could be important when using the W tips as a substrate for fabricating metal-film-coated tips because the electronic or magnetic properties of the covered films are determined by the film crystalline structure.²⁷⁻²⁹ A flat and clean W tip apex is necessary for controlling the film properties, which is in contrast to the motivation for producing an atomically sharp tip. An apex with many atomic defects, such as adatoms, steps, and kinks, destroys the crystalline structures of the deposited film, which was experimentally confirmed by FIM, in which the deposited Fe film on a sharp W tip exhibited amorphous-like structure instead of a bcc symmetry.⁸ Advantages of changing tip apex blunter in a controllable way could be understood by atomic layer stacking models of the apexes with different radii (bcc-W(110), atomic layer distance: 0.223 nm), in Fig. 4(e). These simple models suggest that the apex shape and radius are important for controlling the flat and facet areas at the apex. Here, the "flat" areas are defined as the areas with terraces exceeding 5 nm. For example, a tip with a 5-nm-long terrace has a flat area only within a diameter of 4 nm; however, the flat area diameter increases to more than 30 nm when the radius increases to 40 nm, i.e., to obtain stable electron emission, a tip with $r \gg 5$ nm could be better than an atomically sharp tip.

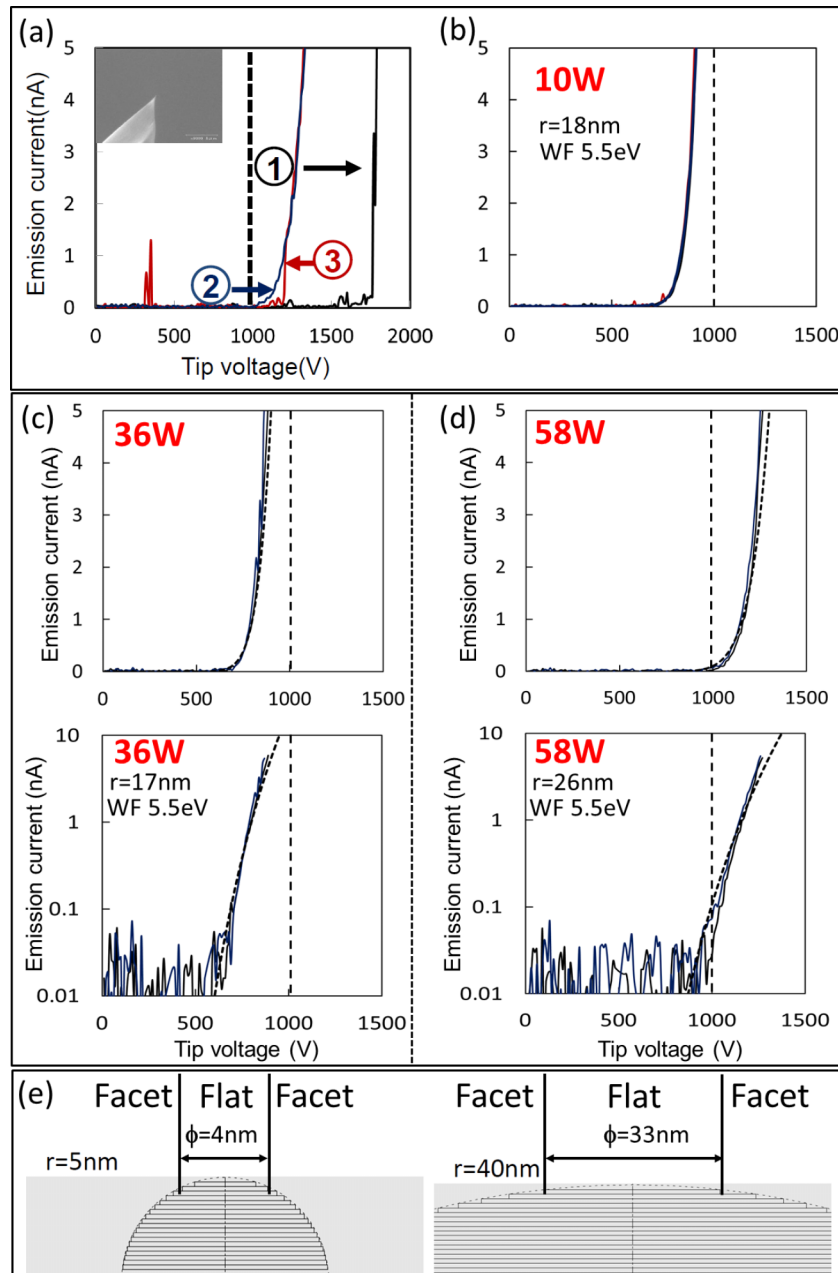


FIG. 4. Experimental field emission I-V curves. The tips were etched from a commercial polycrystalline W wire, and subsequently introduced into the UHV setup. (a) The etched tips exhibited three different curves. (b) After heating by 10 W (10×1), reproducible curves were obtained, yielding the tip radius of 18 nm. (c) Field emission curves obtained from another W tip, yielding the tip radius of 17 nm. The lower panel shows in a log-scale. Solid lines denote experimentally obtained I-V curves and the dashed lines denote fitted curves. (d) After heating by 58 W (10×1), the tip radius increased to 26 nm. The lower panel shows in a log-scale. Solid lines denote experimentally obtained I-V curves and the dashed lines denote fitted curves. (e) Atomic plane models of tip apices for different tip radii. Top atomic layer diameters are shown.

We also tested the tip etched from the long-time heated W wire since the heated wire has larger grains.³⁰ We set the polycrystalline W wire (diameter of 0.3 mm) of Fig. 3 into the UHV chamber and electrically heated the wire (76.7 W for 45 h). Then, the wire was extracted from the UHV chamber, and the wire cross section was polished in air. The cross section's SEM image (Fig. 5(a)) reveals two domains (A and B) with sizes above $100 \mu\text{m}$, i.e., the grain size increased as we expected. We also characterized the crystalline structures by taking X-ray diffraction image (transmitted Debye-Scherrer) obtained by rotating the W wire along the wire axis (Fig. 5(b)). Different from the data in Fig. 3(a), only sharp spots are

observed in Fig. 5(b) (no Debye rings), confirming single crystallization. We repeated to take several Laue images by illuminating X-rays at different positions ($z = 0.0, 0.5, 1.0, 1.5, 2.0, 2.5, 3.0, 3.5$ mm) along the z -axis. As shown in Fig. 5(c), the spot patterns in the Laue images are the same for $z = 0.0$ to $z = 0.5$ mm, but these change from 1.0 mm. Typically, every 1 mm, spot patterns change, indicating that the domain size along the z -axis could be 0.5-1.0 mm.

We etched this wire to obtain a tip. Figure 5(d) shows the tip's SEM image. The surface is not smooth and many edges can be observed. Figure 5(e) shows the top view of the tip's SEM image. The tip had a quadrangular pyramid shape.

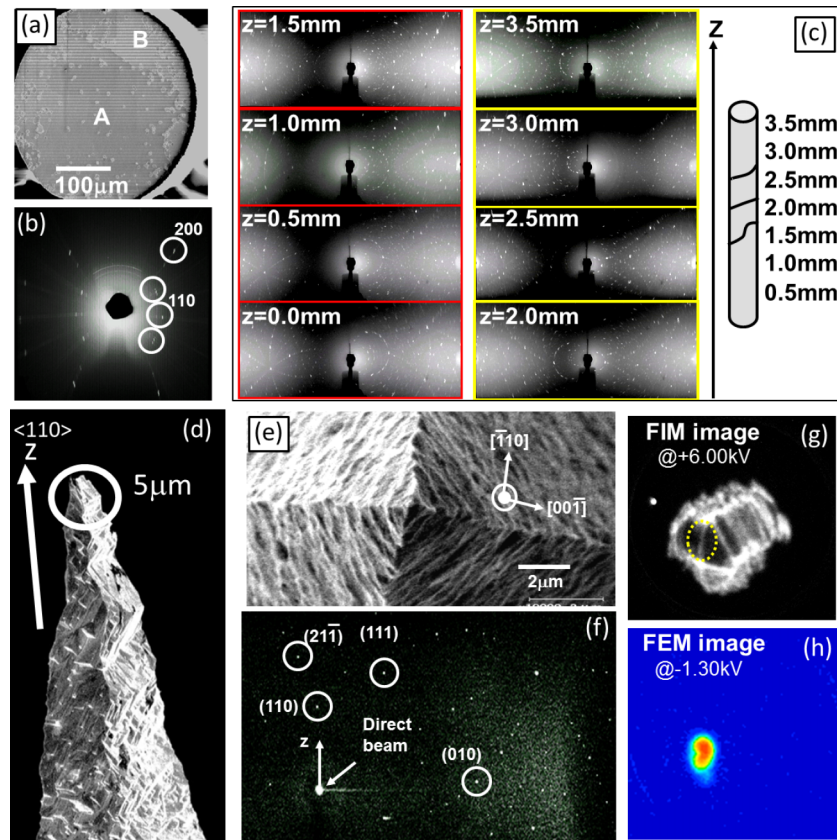


FIG. 5. X-ray, SEM, and FIM/FEM results obtained from the polycrystalline W wire (diameter 0.3 mm) heated by 76.7 W for 45 h and its etched tip. (a) SEM image of a cross section view of the heated wire. Domains A and B are observed. (b) Transmission type X-ray Debye-Scherrer image. (c) X-ray Laue images obtained at different positions along the z -axis. (d) A W tip, chemically etched from the annealed W wire. (e) SEM image observed from the z -axis. (f) X-ray Laue image obtained from the tip apex by illuminating the 5.0 μm region with micro-parabola capillary. ((g) and (h)) FIM (He, 3×10^{-3} Pa) and FEM images ($15 \times 15 \text{ nm}^2$), obtained for the same tip at 300 K. All data were obtained by using an X-ray W tube, 40 kV, 20 mA, exposure time of 120 min.

We illuminated the X-ray only at the tip apex (5 μm) with a micro-parabola capillary. The obtained Laue image in Fig. 5(f) shows the spots, revealing that the $\langle 110 \rangle$ direction is parallel to the z -axis, with deviation contained within one degree. These results indicate that grain boundaries are necessary for fabricating conically shaped tip apices.

This unique shape tip was set into the UHV preparation chamber and I-V measurements performed. Figure 6(a) shows three I-V curves obtained after introducing the tip from air into UHV; all curves are different, similar to the case for the W tip fabricated from the polycrystalline wire (Fig. 4(a)). As shown in Fig. 6(b), after annealing by 10–20 W (10 s \times 1), the

repeatedly obtained I-V curves are identical, suggesting the tip radius of 31 nm. A tip with rather large tip radius could be fabricated by using the electrically heated wire. Same as in Fig. 4, here we tried to determine the threshold heating power for increasing the tip radius. We found that the tip radius started to increase when the power exceeded 40 W. In Fig. 6(c), after annealing by 40 W (10 s \times 1), the resulting I-V curve suggested the tip radius of 37 nm (black). We repeated the I-V measurements. The second curve (red) suggested the tip radius of 36 nm while the third one suggested the tip radius of 40 nm.

We re-fabricated a tip from the electrically heated wire and annealed the tip by 20 W in UHV, following which

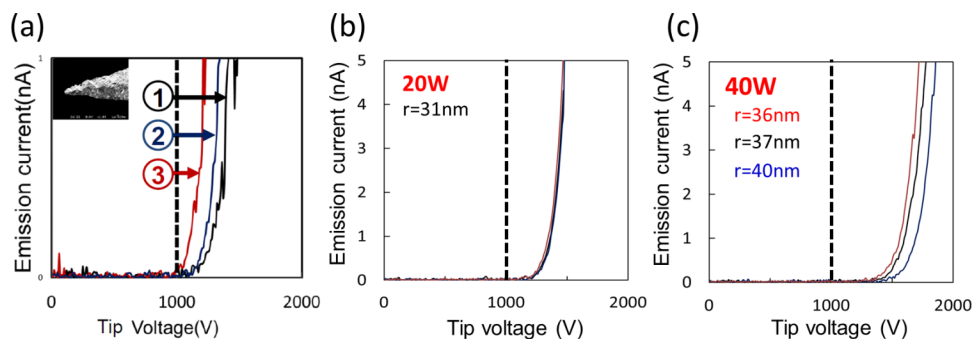


FIG. 6. ((a) and (b)) Field emission I-V curves obtained from the W tip in Fig. 5, before and after heating by 20 W (10 s \times 1). The emission becomes stable after the heating, yielding the tip radius of 31 nm. (c) Further heating, up to 40 W (10 s \times 1), increased the tip radius, while the three curves show 36, 37, and 40 nm.

we performed FIM and FEM measurements (Figs. 5(g) and 5(h)). Although the crystalline orientation was parallel to the bcc-⟨110⟩ direction, the FIM image reveals many 1–3-nm-long atomic steps at the apex, confirming that the apex has many atomic defects. These tips are not as good as a tip with a stable tunneling electron emission. Strong electric fields likely modify the apical atomic structure; therefore, the obtained I–V curves in Fig. 6(c) could be changed in every I–V measurement. Further, if films are deposited on such a tip, the film crystalline structure could become amorphous because no flat atomic planes dominate at the apex.

These results in Fig. 5 suggest that W wires with grain sizes of ~1000 nm should be used for obtaining conically shaped apices with atomic (110) plane, instead of using wires with 0.1–1-mm-size grains, in spite of the fact that the quality of the ⟨110⟩-orientation increases. Comparing the FIM and FEM images, electrons are found to be emitted from one step (marked by the dotted circle in Fig. 5(g)).

CONCLUSIONS

Stable W tips, producing constant tunneling electron emission in the presence of strong electric fields, can be fabricated by excluding impurity layers at the tip apex and producing stable LDOS near the Fermi energy owing to the rigid bcc-⟨110⟩ atomic plane. In this study, we investigated tip preparation methods to obtain the stable W tips. Stability of the electron emission from the tip apex was checked by measuring field emission I–V curves. W tips etched from polycrystalline wires have single crystal grains with a size of ~1000 nm. Electron bombardment heating was used to heat intensively at the apex. 10–40 W heating (lasted 10 s) was required to get stable electron emission; however, heating more than the threshold power (~60 W) started to increase the tip radius (typically +10 nm), which might be useful to grow an atomically flat film with a bcc symmetry (a deposited film on an atomically sharp tip become amorphous). Also, grain size of the wire was found to be an important parameter for determining the shape, i.e., grain size of ~1000 nm is necessary to obtain a conical shape tip apex.

ACKNOWLEDGMENTS

Kind support and discussions with Professor Dr. T. Mizoguchi are acknowledged. This work was supported by

JSPS KAKENHI Grant Nos. 23681018 and 25110011, Asahi Glass Foundation.

- ¹E. W. Müller, *Z. Phys.* **106**, 541 (1937).
- ²E. W. Müller, *Z. Phys.* **131**, 136 (1951).
- ³J. Pawley, *Scanning* **19**, 324 (1997).
- ⁴J. A. Strosio, R. M. Feenstra, and A. P. Fein, *Phys. Rev. Lett.* **57**, 2579 (1986); H. Labidi, M. Kupsta, T. Huff, M. Salomons, D. Vick, M. Taucer, J. Pitters, and R. A. Wolkow, *Ultramicroscopy* **158**, 33 (2015).
- ⁵S. Mizuno, F. Rahman, and M. Iwanaga, *Jpn. J. Appl. Phys., Part 2* **45**, L178 (2006).
- ⁶P. Hommelhoff, C. Kealhofer, and M. A. Kasevich, *Phys. Rev. Lett.* **97**, 247402 (2006).
- ⁷G. A. Fried, X. D. Wang, and K. W. Hipps, *Rev. Sci. Instrum.* **64**, 1495 (1993).
- ⁸T. Irisawa, T. K. Yamada, and T. Mizoguchi, *New J. Phys.* **11**, 113031 (2009).
- ⁹A. I. Oliva, A. G. Romero, J. L. Peña, E. Anguiano, and M. Aguilar, *Rev. Sci. Instrum.* **67**, 1917 (1996).
- ¹⁰O. L. Guise, J. W. Ahner, M.-C. Jung, P. C. Goughnour, and J. T. Yates, Jr., *Nano Lett.* **2**, 191 (2002).
- ¹¹M. Kulakov, I. Luzinov, and K. G. Kornev, *Langmuir* **25**, 4462 (2009).
- ¹²W. T. Chang, I. S. Hwang, M. T. Chang, C. Y. Lin, W. H. Hsu, and J. L. Hou, *Rev. Sci. Instrum.* **83**, 083704 (2012).
- ¹³Y. Khan, H. Al-Falih, Y. Zhang, T. K. Ng, and B. S. Ooi, *Rev. Sci. Instrum.* **83**, 063708 (2012).
- ¹⁴I. Ekvall, E. Wahlstrom, D. Claesson, H. Olin, and E. Olsson, *Meas. Sci. Technol.* **10**, 11 (1999).
- ¹⁵G. J. de Raad, P. M. Koenraad, and J. H. Wolter, *J. Vac. Sci. Technol., B: Microelectron. Nanometer Struct.* **17**, 1946 (1999).
- ¹⁶A.-S. Lucier, H. Mortensen, Y. Sun, and P. Grütter, *Phys. Rev. B* **72**, 235420 (2005).
- ¹⁷J. Onoda and S. Mizuno, *Appl. Surf. Sci.* **257**, 8427 (2011).
- ¹⁸J. Onoda, S. Mizuno, and H. Ago, *Surf. Sci.* **604**, 1094 (2010).
- ¹⁹C. Vesa, R. Urban, J. L. Pitters, and R. A. Wolkow, *Appl. Surf. Sci.* **300**, 16 (2014).
- ²⁰A. N. Chaika, N. N. Orlova, V. N. Semenov, E. Yu. Postnova, S. A. Krasnikov, M. G. Lazarev, S. V. Chekmazov, V. Yu. Aristov, V. G. Glebovsky, S. I. Bozhko, and I. V. Shvets, *Sci. Rep.* **4**, 3742 (2014).
- ²¹M. M. J. Bischoff, T. K. Yamada, C. M. Fang, R. A. de Groot, and H. van Kempen, *Phys. Rev. B* **68**, 045422 (2003).
- ²²L. A. Hockett and S. E. Creager, *Rev. Sci. Instrum.* **64**, 263 (1993).
- ²³T. K. Yamada, M. M. J. Bischoff, G. M. M. Heijnen, T. Mizoguchi, and H. van Kempen, *Phys. Rev. Lett.* **90**, 056803 (2003).
- ²⁴A. Cricenti, E. Paparazzo, M. A. Scarselli, L. Moretto, and S. Selci, *Rev. Sci. Instrum.* **65**, 1558 (1994).
- ²⁵A.-D. Müller, F. Müller, M. Hietschold, F. Demming, J. Jersch, and K. Dickmann, *Rev. Sci. Instrum.* **70**, 3970 (1999).
- ²⁶R. S. Polizzotti and G. Erhlich, *Surf. Sci.* **91**, 24 (1980).
- ²⁷S. Schmaus, A. Bagrets, Y. Nahas, T. K. Yamada, A. Bork, F. Evers, and W. Wulfhekel, *Nat. Nanotechnol.* **6**, 185 (2011).
- ²⁸A. Bagrets, S. Schmaus, A. Jaafar, D. Kramczynski, T. K. Yamada, M. Alouani, W. Wulfhekel, and F. Evers, *Nano Lett.* **12**, 5131 (2012).
- ²⁹T. K. Yamada and A. L. Vazquez de Parga, *Appl. Phys. Lett.* **105**, 183109 (2014).
- ³⁰M. Greiner and P. Kruse, *Rev. Sci. Instrum.* **78**, 026104 (2007).